Nonlinear mobile sensor calibration using informed semi-nonnegative matrix factorization with a Vandermonde factor

Clément Dorffer, Matthieu Puigt, Gilles Delmaire, Gilles Roussel

NONLINEAR MOBILE SENSOR CALIBRATION USING INFORMED SEMI-NONNEGATIVE MATRIX FACTORIZATION WITH A VANDERMONDE FACTOR

Clément Dorffer, Matthieu Puigt, Gilles Delmaire, and Gilles Roussel

Univ. Littoral Côte d'Opale, EA 4491 – LISIC, F-62228 Calais, France

ABSTRACT

In this paper we aim to blindly calibrate a mobile sensor network whose sensor outputs and the sensed phenomenon are linked by a polynomial relationship. The proposed approach is based on a novel informed semi-nonnegative matrix factorization with a Vandermonde factor matrix. The proposed approach outperforms a matrix-completion-based method in a crowdsensing-like simulation of particulate matter sensing.

***Index Terms*—** nonlinear sensor calibration, informed semi-NMF, structured matrix factorization

1. INTRODUCTION

Crowdsensing consists of acquiring some geolocalized and time-stamped data from a crowd of mobile sensors provided by mobile devices, e.g., smartphones [1]. However, crowdsensing sensors are usually low cost and must be oftenly calibrated in the wild, as it may not be possible to request them to regularly go to a laboratory. To deal with such an issue, specific blind sensor calibration methods have been proposed. Such techniques are usually divided into two main families, namely micro- and macro-calibration. Micro-calibration consists of independently calibrating each sensor of a network while macro-calibration operates on the whole set of sensors [2]. Most blind calibration approaches allow to tackle gain [3, 4], gain/offset [5, 6, 7, 8, 9], gain/phase [10, 11] calibration, and sensor drift [12]. When the sensors of the network can move, Blind Mobile Sensor Calibration (BMSC) techniques are usually exploiting the *rendezvous* model [13] which assumes that sensors in the same spatio-temporal vicinity should acquire the same data. Contrary to [12], the authors in [6, 7, 8, 9] consider the situation when some sensors are perfectly calibrated, thus helping the calibration of the rest of the sensor network. In particular, the work in [6, 7] proposes a multi-hop micro-calibration structure. That is, calibrated sensors are used to calibrate uncalibrated ones which lie in the same vicinity. These sensors are then considered as calibrated and used to calibrate other ones when they move. The operation is then repeated until any sensor in the network is calibrated. On the contrary, our previous work in [8, 9] is based on macro-calibration and is revisiting BMSC as an informed Nonnegative Matrix Factorization (NMF) problem. Our approaches are assuming a nonnegative affine calibration function, which is valid for a limited number of sensors only.

In this paper, we extend our previous work by proposing a novel nonlinear calibration method where the nonlinear function is assumed to be polynomial. Interestingly, while being extremely general, such a model for BMSC has been considered in a very limited number of papers, i.e., [14, 15]. The work in [14] also considers a polynomial calibration function and proposes two BMSC approaches based on nullspace—i.e., an extension of [5]—and on moments, respectively. The work in [15] considers an extended moment-based calibration method, where the nonlinear calibration function is assumed to be piecewise linear. However, it should be noticed that the nullspace-based method is very sensitive to noise [14] and needs some knowledge on the *true* subspace where the sensed data should lie. The moment-based calibration approach is more robust to noise but it needs a very long integration time to perform an accurate calibration [14, 15]. On the contrary, the method we propose in this paper—which is extending our previous work—is based on an informed semi-NMF framework and neither requests the exact knowledge of the sensed data subspace nor needs a long integration time.

The remainder of this paper is organized as follows. We introduce the nonlinear BMSC problem in Section 2 and our proposed approach in Section 3. Its experimental performance is investigated in Section 4 while we conclude and discuss about future work in Section 5.

2. PROBLEM STATEMENT

In this paper we consider a set of m heterogeneous, geolocalized, time-stamped, mobile, and possibly uncalibrated sensors to provide measurements over a fixed area and over time. We now introduce the definitions used in this paper.

Definition 1 ([13]) *A* rendezvous *is a temporal and spatial vicinity between two sensors.*

A rendezvous is characterized by a time interval Δ_t and a spatial distance Δ_d which depend on the observed phenomenon.

Definition 2 ([8]) *A* scene $\mathcal{S}$ *is a discretized area observed during a time interval* $[t, t+\Delta_t)$*. The size of the spatial pixels*

This work was funded by the "OSCAR" project within the Région Hauts-de-France "Chercheurs Citoyens" Program.

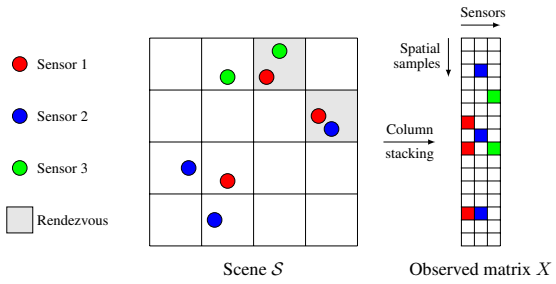

Fig. 1. From a scene $\mathcal{S}$ (with $n = 16$ spatial samples, $m = 3$ sensors and 2 rendezvous) to the data matrix X (white pixels mean no observed value).

are set so that any couple of points inside the same pixel have a distance below Δ_d.

As shown in Fig. 1, a scene is a grid of locations where the sensors go to. When two sensors share the same location in $\mathcal{S}$, they are in rendezvous and should acquire the same data.

The sensor output $x_{i,j}$—provided by Sensor j at Location i of a scene $\mathcal{S}$—is linked to the corresponding physical value—denoted y_i—through a nonlinear calibration function $\mathcal{F}_j$ accurately inferred by a polynomial (of degree N), i.e.,

$$x_{i,j} \approx \mathcal{F}_j(y_i) \approx f_{1,j} + f_{2,j} \cdot y_i + \cdots + f_{N+1,j} \cdot y_i^N, \quad (1)$$

where the $f_{k,j}$ terms are the calibration parameters associated with Sensor j. Please note that such a relationship is extending the affine calibration model [8, 9] as the latter is derived from Eq. (1) by assuming that $f_{k,j} = 0$ for $k \geq 3$.

Assuming a scene composed of n locations and fully observed by m nonlinear mobile sensors (with $\min(n, m) \gg N$), we respectively define the $n \times (N+1)$ and $(N+1) \times m$ matrices G and F as

$$G \triangleq \begin{bmatrix} 1 & y_1 & \cdots & y_1^N \\ \vdots & \vdots & & \vdots \\ 1 & y_n & \cdots & y_n^N \end{bmatrix}, F \triangleq \begin{bmatrix} f_{1,1} & \cdots & f_{1,m} \\ \vdots & & \vdots \\ f_{N+1,1} & \cdots & f_{N+1,m} \end{bmatrix}, \quad (2)$$

and we derive the matrix form of Eq. (1), i.e.,

$$X \approx G \cdot F, \quad (3)$$

where $X \triangleq [x_{i,j}]_{i,j}$ is a low-rank well-conditionned matrix. G is a Vandermonde matrix—denoted $G \triangleq \text{VDM}(\underline{y}, N)$ below—whose columns provide the monomial expansion of the sensed physical values $\underline{y} \triangleq [y_1, \ldots, y_m]^T$ while F contains the calibration parameters.

It should be noticed that estimating both G and F from X is a specific nonlinear matrix factorization problem, which has never been investigated to the best of the authors' knowledge. Indeed, most nonlinear matrix factorization approaches were proposed for bilinear source separation [16, 17, 18], whose nonlinear dependencies in one matrix factor are different from the Vandermonde factor considered in this paper[1].

[1]However [19] considers a Vandermonde factor in tensor factorization.

As the sensors are unconstrained in their moves, none might sense the whole scene, thus leading to missing values which are taken into account by applying a binary mask W—informing the presence/absence of data in X—on the factorization, i.e., denoting $\circ$ the Hadamard product:

$$W \circ X \approx W \circ (G \cdot F), \quad (4)$$

Lastly, we assume that X and G are nonnegative, which is a valid assumption in many environmental applications[2]. Moreover, we assume that one sensor—say Sensor m—is calibrated and that its calibration parameters read

$$f_{2,m} = 1 \text{ and } f_{k,m} = 0 \text{ if } k \neq 2. \quad (5)$$

This implies that an available data point in the last column of X—say $x_{i,m}$—is equal to the sensed phenomenon y_i in the second column of G. Since G is a Vandermonde matrix, its monomial expansions are known too, i.e., the whole i-th row of G is known. As a consequence, we get some knowledge on both G and F that may help to enhance the factorization (and in particular, to suppress the scale ambiguity inherent to matrix factorization and that we must avoid to perform sensor calibration). Using the parameterization proposed in [20], we rewrite G and F with respect to their set and free parts, i.e.,

$$G \triangleq \Omega_G \circ \Phi_G + \bar{\Omega}_G \circ \Delta_G, \quad F \triangleq \Omega_F \circ \Phi_F + \bar{\Omega}_F \circ \Delta_F, \quad (6)$$

where Ω_G (respectively, Ω_F) is a binary matrix informing the presence/absence of constraints in G (respectively, F), Φ_G (respectively, Φ_F) is the matrix containing the set entries in G (respectively, F), Δ_G (respectively, Δ_F) is the matrix of the free parameters in G (respectively, F), and $\bar{\Omega}_G \triangleq \mathbb{1}_{n\times(N+1)} - \Omega_G$ (respectively, $\bar{\Omega}_F \triangleq \mathbb{1}_{(N+1)\times m} - \Omega_F$), where $\mathbb{1}_{i\times j}$ is the $i \times j$ matrix of ones.

In this paper, we thus aim to estimate F (and G) from:

$$\begin{aligned} \{\hat{G}, \hat{F}\} \quad = \quad & \arg\min_{G,F} ||W \circ (X - G \cdot F)||_{\mathcal{F}}^2 \\ \text{s.t.} \quad & G = \text{VDM}(\underline{y}, N) \geq 0, \\ & G = \Omega_G \circ \Phi_G + \bar{\Omega}_G \circ \Delta_G, \\ & F = \Omega_F \circ \Phi_F + \bar{\Omega}_F \circ \Delta_F, \end{aligned} \quad (7)$$

which is possible, provided enough diversity in $\underline{y}$ and F.

3. PROPOSED APPROACH

As Eq. (7) is non-convex w.r.t. both G and F, we split it into

$$\begin{aligned} \hat{G} \quad = \quad & \arg\min_{G} ||W \circ (X - G \cdot F)||_{\mathcal{F}}^2 \\ \text{s.t.} \quad & G = \text{VDM}(\underline{y}, N) \geq 0, \\ & G = \Omega_G \circ \Phi_G + \bar{\Omega}_G \circ \Delta_G, \end{aligned} \quad (8)$$

and

$$\begin{aligned} \hat{F} \quad = \quad & \arg\min_{F} ||W \circ (X - G \cdot F)||_{\mathcal{F}}^2 \\ \text{s.t.} \quad & F = \Omega_F \circ \Phi_F + \bar{\Omega}_F \circ \Delta_F, \end{aligned} \quad (9)$$

which then can be alternately and iteratively solved, as explained in Subsections 3.1 and 3.2, respectively.

[2]$x_{i,j}$ and y_i may respectively represent a voltage and a concentration [8].

3.1. Updating strategy for the Vandermonde matrix G

From the parameterization (6), it should be noticed that only the free part of G, i.e., Δ_G, has to be updated in the optimization problem (8). The associated cost function then reads

$$\mathcal{J}_G(\Delta_G) = \sum_{i=1}^{m}\sum_{j=1}^{n} W_{i,j}^2 \cdot \left(\tilde{X}_{i,j} - ((\bar{\Omega}_G \circ \Delta_G)\cdot F)_{i,j}\right)^2, \tag{10}$$

where $\tilde{X} \triangleq X - (\Omega_G \circ \Phi_G)\cdot F$. As explained above, if a value of $\underline{y}$ is known, then all the corresponding line of G is set in Φ_G. On the contrary, when a value—say y_i—is unknown, then all the i-th row of G must be estimated, i.e., the i-th row of Δ_G must be updated. Expressing Eq. (10) with respect to $\Delta_{\underline{y}}$—the second column of Δ_G—reads

$$\mathcal{J}_G(\Delta_{\underline{y}}) = \sum_{i=1}^{m}\sum_{j=1}^{n} W_{i,j}^2 \cdot \left(\tilde{X}_{i,j} - \sum_{k=0}^{N} (\bar{\Omega}_G)_{i,k}\cdot(\Delta_{\underline{y}})_i^k \cdot F_{j,k}\right)^2. \tag{11}$$

Using this last expression, we propose a two-step update of the whole matrix G which first consists of updating $\Delta_{\underline{y}}$ using one iteration of a projected gradient descent—in order to respect the data nonnegativity—and then propagating[3] this updated column into G so as to respect the Vandermonde structure (2). Deriving the cost function (11) yields to

$$\nabla\mathcal{J}_G(\Delta_{\underline{y}}) = \text{diag}\left[(W^2 \circ Z)\cdot(F^s)^T \cdot (\bar{\Omega}_G^s \circ U \circ \Delta_G^s)^T\right], \tag{12}$$

where $Z \triangleq (\bar{\Omega}_G \circ \Delta_G)\cdot F - \tilde{X}$, U is a $N \times N$ matrix whose (i,j)-th element $u_{ij} \triangleq j$, $W^2 \triangleq W \circ W$, $\bar{\Omega}_G^s$ is the matrix composed of the $N-1$ last columns of $\bar{\Omega}_G$, Δ_G^s is the matrix composed of the $N-1$ first columns of Δ_G and F^s is the matrix composed of the $N-1$ last rows of F. The projected gradient descent update then reads

$$\Delta_{\underline{y}} \leftarrow \left[\Delta_{\underline{y}} - \lambda_G \cdot \nabla\mathcal{J}_G(\Delta_y)\right]^+, \tag{13}$$

where λ_G is the descent step size for G and $[.]^+$ is the projection operator on $\mathbb{R}^+$.

3.2. Updating strategy for the parameter matrix F

Using the parameterization (6), the cost function (9) can be expressed with respect to Δ_F as

$$\mathcal{J}_F(\Delta_F) = \sum_{i=1}^{m}\sum_{j=1}^{n} W_{i,j}^2 \cdot \left(\tilde{\tilde{\mathrm{X}}}_{i,j} - (G\cdot(\bar{\Omega}_F \circ \Delta_F))_{i,j}\right)^2, \tag{14}$$

where $\tilde{\tilde{\mathrm{X}}} \triangleq X - G\cdot(\Omega_F \circ \Phi_F)$. Its gradient reads

$$\nabla\mathcal{J}_F(\Delta_F) = \bar{\Omega}_F \circ \left[G^T \cdot \left(W^2 \circ \left(G\cdot(\bar{\Omega}_F \circ \Delta_F)\right) - \tilde{\tilde{\mathrm{X}}}\right)\right]. \tag{15}$$

[3] A similar strategy was proposed in [16, 18] in a linear-quadratic (nonnegative) matrix factorization framework.

As F is not subject to any sign constraint, we thus propose to update it by one gradient descent step which leads to

$$\Delta_F \leftarrow \Delta_F - \lambda_F \cdot \nabla\mathcal{J}_F(\Delta_F), \tag{16}$$

where λ_F is the descent step size for F.

3.3. Algorithmic strategies

We here discuss some implementation issues which were met in some preliminary tests. As the proposed method is iterative, it should be initialized. We follow a similar strategy as in [8], i.e., we first apply matrix completion [21] to X. Using its completed version, we derive from Eqs. (5) and (2) an estimation of $\underline{y}$ and G, respectively. A naive calibration—which was used to initialize the approach in [8]—consists of estimating F by least squares. However, the semi-NMF with this initialization did not always provide a good enhancement. On the contrary, initializing F with random realizations around known theoretical average values—which are provided by the sensor manufacturer—was found to be a better strategy.

A tricky aspect of the proposed gradient-based method is the choice of the step sizes λ_G and λ_F, respectively introduced in Eqs. (13) and (16). Indeed, if these step sizes are too small, the proposed approach needs a lot of iterations to converge, which is time consuming. On the contrary, if it is too big, the projection in the update of G tends to be massively applied, hence providing a very poor performance along iterations. Moreover, we found in preliminary tests that choosing well-suited step sizes is also depending of the missing data proportion[4]. We thus found from preliminary tests a trade-off by setting step sizes varying with the missing value proportion ρ in X, i.e.,

$$\lambda_G = 0.001(\rho + 0.1), \quad \lambda_F = 0.01(\rho + 0.1). \tag{17}$$

4. EXPERIMENTAL VALIDATION

In this section, we aim to investigate the enhancement provided by our proposed informed nonlinear Semi-NMF method for BMSC. For that purpose, we simulate a crowdsensing-like particulate matter sensing during a time interval $[t, t+\Delta_t)$, which satisfies the assumptions in Section 2. The scene is a 10×10 discretized area (the length of $\underline{y}$ is thus equal to $n = 100$) which is observed by $m = 31$ sensors, i.e., $m-1$ uncalibrated and mobile dust sensors [22] and one calibrated, high quality, and mobile sensor[5].

The observed concentrations in $\underline{y}$ range from 1e-3 to 1.4 mg/m^3, for which the nonlinear sensor response is accurately inferred by a polynomial of degree $N = 2$ [22].

[4] Ideally, the optimal step size should be estimated within iterations. However, such an estimation is non-trivial for the Vandermonde factor and out of the scope of this paper.

[5] Actually, we get k fixed, calibrated, and highly accurate sensors whose outputs are modeled as those of the m-th sensor in the BMSC problem.

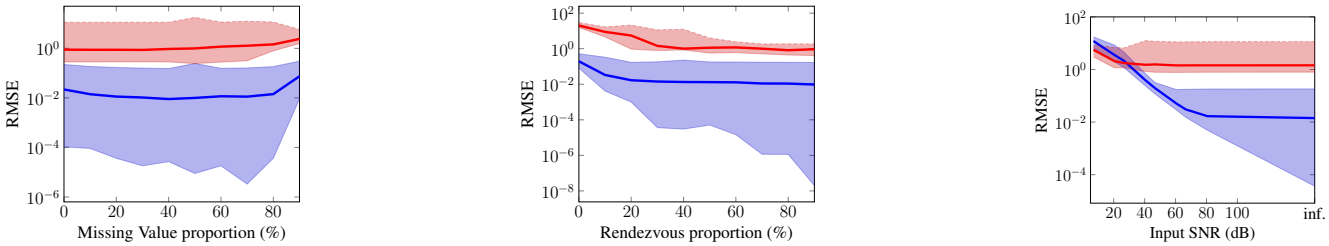

Fig. 2. BMSC performance vs *(left)* the missing value proportion, *(center)* the rendezvous proportion, and *(right)* the input SNR. Perf. criterion: RMSE.

In particular, following the datasheet [22], for each index $j = 1, \ldots, m-1$, the calibration parameters $f_{1,j}$, $f_{2,j}$, and $f_{3,j}$—defined in Eq. (1)—of the uncalibrated mobile sensors are randomly set according to a Gaussian distribution centered around 0.9, 13, and -2.5, respectively. We then get a 31×100 theoretical observation matrix for which we randomly keep $k + l$ samples, where k (respectively, l) is the number of calibrated (respectively, uncalibrated) sensor samples—with $k \ll l$—hence providing the irregular sampling over the scene. Lastly, Gaussian noise realizations may be added to the observed uncalibrated sensor data.

In this section, we aim to investigate the performance of the number of rendezvous between calibrated and uncalibrated sensors, the number of missing entries in X, and the influence of the input SNR to the BMSC performance. For each test condition—i.e., one number of rendezvous, one proportion of missing entries, or one input SNR—20 simulations are performed. For each run, we randomly set the position of the samples in X in the three experiments and we generate different noise realizations in the last one. The number k of calibrated sensor values in the m-th column of X is set to 4 in all the tests. Except when we make these values vary, the proportion of uncalibrated sensors to have rendezvous with calibrated ones, and the proportion of missing entries in X are set to 30 and 80 %, respectively. In addition to the noiseless case, the input SNR varies from 10 to 80 dB. Lastly, the runs are stopped after 5e5 iterations. The estimation error of each calibration parameter is measured by the Root Mean Square Error (RMSE) computed between a row of true parameters in F and the corresponding row of reconstructed ones. Their average provides a global RMSE for the considered simulation. It should be noticed that state-of-the-art nonlinear calibration methods [14, 15] cannot be tested in this experimental section, because they require the observed signal subspace knowledge and/or some time synchronization of the sensors measurements—which is a strong assumption not satisfied in most crowdsensing applications, and not needed by the proposed method.

Figure 2 shows the plots of the different experiments realized in this paper. The blue (respectively, red) line corresponds to the median RMSE obtained with our proposed method (respectively, the matrix-completion-based approach discussed in Subsection 3.3) applied on 20 independent tests while the blue (respectively, red) area shows the envelope of the RMSEs obtained with our proposed method (respectively, the matrix-completion-based approach). The left plot shows the influence of the proportion ρ of missing values—ranging from 0.1 to 0.9—on the obtained RMSE. Our proposed method always outperforms the naive approach. Interestingly, the median RMSE is very stable with respect to ρ: it slightly increases when $\rho = 90$ % only. Lastly, it seems strange that the low part of the envelope is almost decreasing when ρ increases (until 70 %). In fact, in several simulations, the semi-NMF method did not converge to the optimal solution within 5e5 iterations, which should be solved by running more iterations. The central plot shows the influence of the number rendezvous between calibrated and uncalibrated sensors. Again, the proposed method outperforms the naive approach and provides stable median RMSEs over the rendezvous proportion. Strangely, the RMSE is not that high when there is no rendezvous. In fact, the factorization is obtained up to a scale ambiguity and, since the initialization is not too far from the true values, the RMSE remains quite low. The right plot shows the influence of the input SNR on the performance. The proposed approach outperforms the naive method if the input SNR is above 35 dB. It should provide a better performance at lower input SNRs with more data points, e.g., by considering several scenes and by stacking the data matrices into a unique bigger one.

5. CONCLUSION

In this paper, we proposed an informed nonlinear semi-NMF method for mobile sensor calibration. The proposed approach is using a Vandermonde structure in one factor and is able to process the factorization with missing data. The proposed method was tested on a crowdsensing-like simulation and was found to provide a stable median performance over the missing value proportion and the number of rendezvous between calibrated and uncalibrated sensors. In future work, we aim to speed up the proposed approach, e.g., by estimating optimal gradient step-sizes. Moreover, we aim to consider other nonlinear calibration functions, e.g., to deal with sensor response drift or saturation.

6. REFERENCES

[1] R. K. Ganti, F. Ye, and H. Lei, "Mobile crowdsensing: current state and future challenges," *Communications Magazine, IEEE*, vol. 49, no. 11, pp. 32–39, Nov. 2011.

[2] K. Whitehouse and D. Culler, "Macro-calibration in sensor/actuator networks," *Mobile Networks and Applications*, vol. 8, no. 4, pp. 463–472, Aug. 2003.

[3] H. Carfantan and J. Idier, "Statistical linear destriping of satellite-based pushbroom-type images," *IEEE Trans. on Geoscience and Remote Sensing*, vol. 48, no. 4, pp. 1860–1871, Apr. 2010.

[4] C. Schulke, F. Caltagirone, F. Krzakala, and L. Zdeborova, "Blind calibration in compressed sensing using message passing algorithms," in *NIPS 26*, 2013, pp. 566–574.

[5] L. Balzano and R. Nowak, "Blind calibration of sensor networks," in *Proc. of IPSN*, 2007, pp. 79–88.

[6] E. Miluzzo, N. D. Lane, A. T. Campbell, and R. Olfati-Saber, "CaliBree: A self-calibration system for mobile sensor networks," in *Proc. of DCOSS*, 2008, vol. 5067 of *LNCS*, pp. 314–331.

[7] O. Saukh, D. Hasenfratz, and L. Thiele, "Reducing multi-hop calibration errors in large-scale mobile sensor networks," in *Proc. of IPSN*, 2015.

[8] C. Dorffer, M. Puigt, G. Delmaire, and G. Roussel, "Blind calibration of mobile sensors using informed nonnegative matrix factorization," in *Proc. of LVA-ICA*, vol. 9237 of *LNCS*, pp. 497–505. 2015.

[9] C. Dorffer, M. Puigt, G. Delmaire, and G. Roussel, "Blind mobile sensor calibration using a nonnegative matrix factorization with a relaxed rendezvous model," in *Proc. of ICASSP*, Mar. 2016.

[10] P. H. Schönemann, "On metric multidimensional unfolding," *Psychometrika*, vol. 35, no. 1, pp. 349–366, Mar. 1970.

[11] C. Bilen, G. Puy, R. Gribonval, and L. Daudet, "Convex optimization approaches for blind sensor calibration using sparsity," *IEEE Trans. Signal Processing*, vol. 62, no. 18, pp. 4847–4856, Sept. 2014.

[12] B.-T. Lee, S.-C. Son, and K. Kang, "A blind calibration scheme exploiting mutual calibration relationships for a dense mobile sensor network," *IEEE Sensors Journal*, vol. 14, no. 5, pp. 1518–1526, May 2014.

[13] O. Saukh, D. Hasenfratz, C. Walser, and L. Thiele, "On rendezvous in mobile sensing networks," in *Proc. of REALWSN*, 2014, vol. 281 of *LNCS*, pp. 29–42.

[14] C. Wang, P. Ramanathan, and K. K. Saluja, "Calibrating nonlinear mobile sensors," in *Proc. of SECON*, Jun. 2008, pp. 533–541.

[15] C. Wang, P. Ramanathan, and K. K. Saluja, "Blindly calibrating mobile sensors using piecewise linear functions," in *Proc. of SECON*, Jun. 2009, pp. 1–9.

[16] I. Meganem, Y. Deville, S. Hosseini, P. Déliot, and X. Briottet, "Linear-quadratic blind source separation using NMF to unmix urban hyperspectral images," *IEEE Trans. Signal Processing*, vol. 62, no. 7, pp. 1822–1833, Apr. 2014.

[17] C. Févotte and N. Dobigeon, "Nonlinear hyperspectral unmixing with robust nonnegative matrix factorization," *IEEE Trans. Image Processing*, vol. 24, no. 12, pp. 4810–4819, Dec. 2015.

[18] Y. Deville, "Matrix factorization for bilinear blind source separation: Methods, separability and conditioning," in *Proc. of EUSIPCO*, Aug. 2015, pp. 1900–1904.

[19] M. Sørensen and L. De Lathauwer, "Blind signal separation via tensor decomposition with Vandermonde factor: Canonical polyadic decomposition," *IEEE Trans. Signal Processing*, vol. 61, no. 22, pp. 5507–5519, Nov. 2013.

[20] A. Limem, G. Delmaire, M. Puigt, G. Roussel, and D. Courcot, "Non-negative matrix factorization under equality constraints—a study of industrial source identification," *Applied Numerical Mathematics*, vol. 85, pp. 1–15, Nov. 2014.

[21] S. R. Becker, E. J. Candès, and M. C. Grant, "Templates for convex cone problems with applications to sparse signal recovery," *Math. Progr. Comp.*, vol. 3, no. 3, pp. 165–218, 2011.

[22] B+B Sensors Corp., "STBM 271 dust sensor module," May 2014, Datasheet.